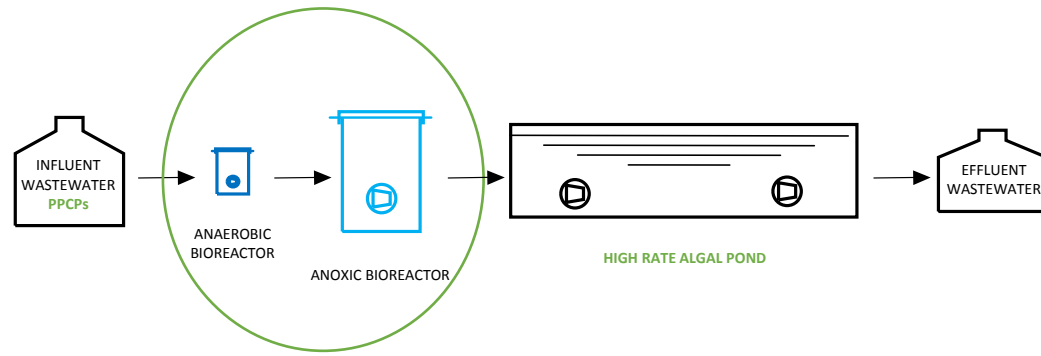


***Graphical Abstract**



Research highlights

- This work evaluated the removal of ECs in novel AX-HRAP and ANA-AX-HRAP PBRs
- Triclosan and propylparaben showed total elimination during ANA-AX-HRAP set-up
- REs > 90% were obtained for ibuprofen and salicylic acid in the ANA-AX-HRAP PBR
- Naproxen was the most recalcitrant with eliminations rates below 52% in all cases
- Biodegradation and sorption were hypothesized as main removal mechanisms

1 **Removal of contaminants of emerging concern from urban wastewater in**
2 **novel algal-bacterial photobioreactors**

3
4 Rebeca López-Serna^{*1,2}, Esther Posadas^{1,2}, Pedro A. García Encina^{1,2}, Raúl Muñoz^{1,2}

5 Department of Chemical Engineering and Environmental Technology, School of Industrial
6 Engineerings, Valladolid University, Dr. Mergelina, s/n, 47011, Valladolid, Spain

7 Institute of Sustainable Processes (IPS), Valladolid University, Dr. Mergelina, s/n, 47011,
8 Valladolid, Spain

9 *corresponding author: rebeca.lopezserna@iq.uva.es

10

11 **ABSTRACT**

12 This work evaluates the removal of five pharmaceuticals and personal care products, i.e.,
13 ibuprofen, naproxen, salicylic acid, triclosan and propylparaben, from urban wastewater
14 under two novel algal-bacterial photobioreactor settings. The first configuration (phase A)
15 consisted of an anoxic-aerobic photobioreactor operating at a hydraulic retention time
16 (HRT) of 2 d at different concentrations of total organic carbon (TOC) (90 mg L^{-1} – 200 mg
17 L^{-1}). In the second configuration (phase B) an anaerobic step was introduced before the
18 anoxic tank to set a photosynthetic A_2O process. In this phase, the HRT varied between 3

19 and 4 d and the TOC was kept constant at 200 mg L⁻¹. In addition, the impact of external
20 aeration in the aerobic photobioreactor was assessed. The maximum removals for
21 ibuprofen, naproxen, salicylic acid, triclosan and propylparaben (94±1%, 52±43%, 98±2%,
22 100±0%, 100±0%, respectively) were recorded during phase B. In phase A, low TOC
23 concentrations triggered higher ibuprofen and naproxen removals likely due to the high
24 contribution of biological oxidation on their removal. In phase B, total or very high
25 removal efficiencies were observed for ibuprofen, propylparaben and triclosan
26 independently on the operating conditions. In contrast, the removal efficiency of
27 naproxen and salicylic acid decreased when the HRT dropped from 4 to 3 d in the absence
28 of external aeration, which suggests that biodegradation played a key role in their
29 removal. In addition, sorption might have contributed to the elimination of triclosan and
30 propylparaben from the wastewater.

31

32 **Keywords:**

33 Algal-bacterial processes; emerging pollutants; microalgae; microcontaminants;
34 micropollutants; PPCPs; wastewater treatment.

35

36

37

38

39 **1. Introduction**

40 Multiple organic compounds initially present in pharmaceuticals, personal care products,
41 plasticizers, surfactants and pesticides are daily released into the environment via
42 wastewater discharge from conventional wastewater treatment plants (WWTPs), which
43 were not originally designed for the removal of such recalcitrant compounds (Matamoros
44 et al., 2015; Rivera-Utrilla et al., 2013). These pollutants are referred to as contaminants of
45 emerging concern (CECs), and their pernicious effects on the environment and human
46 health are still unknown (although reproductive disruption in fish and other aquatic
47 organisms such as alligators and frogs has been reported (Orlando and Ellestad, 2014))
48 (Alan et al., 2008). In this context, and despite the lack of regulatory limits of discharge of
49 CECs into natural water bodies, the recent Directive (2013/39/EU) (European Commission,
50 2013) has updated the previous list of 41 priority substances to 45, which has boosted
51 research on cost-effective methods for CEC removal. Conventional physical-chemical
52 technologies such as adsorption on activated carbon and advanced oxidation processes
53 (i.e. ozonation, photooxidation, radiolysis and electrochemical oxidation) have been
54 tested both at lab and industrial scale to remove CECs from wastewaters. However, the
55 tentative toxicity of the resulting transformation products and the lack of consistent
56 analytical data together with the high investment and operating costs of these
57 technologies has limited their application in WWTPs (Rivera-Utrilla et al., 2013). In this
58 context, algal-bacterial processes have recently emerged as a cost-effective and

59 environmentally friendly alternative to remove CECs from wastewaters (Norvill et al.,
60 2016). Microalgae-based wastewater treatment is based on the solar-driven conversion of
61 carbon and nutrients from wastewater into algal-bacterial biomass (de Godos et al., 2012;
62 Hom-Diaz et al., 2017a; Matamoros et al., 2015; Norvill et al., 2016). Although this green
63 technology was not originally engineered to remove CECs from wastewaters, process
64 operation at high sludge retention time (4-20 d), the enhanced penetration of UV light as
65 a result of their high surface area to volume ratios, and the high daily variations of pH (7-
66 11), dissolved oxygen concentration (2-25 mg O₂ L⁻¹) and temperature (depending on the
67 climatic zone) render algal-bacterial photobioreactors a promising platform for the
68 removal of CECs (Hom-Diaz et al., 2017a; Matamoros et al., 2015; Norvill et al., 2016;
69 Norvill et al., 2017). Thus, (Matamoros et al., 2015) evaluated the effect of the hydraulic
70 retention time (HRT) on the removal of 26 CECs from urban wastewater in two outdoor
71 high rate algal ponds (HRAPs) of 470 L and concluded that up to 90% of the contaminant
72 risk was removed during microalgae-based treatment. More recently, (Hom-Diaz et al.,
73 2017a) recorded removal efficiencies above 48% in 17 pharmaceuticals detected in toilet
74 wastewater and treated by a pilot-scale HRAP working at a HRT of 8 and 12 d. Similarly,
75 (Norvill et al., 2017) and (de Godos et al., 2012) reported tetracycline removal efficiencies
76 (REs) of 93% and 69±1% in a 180-L outdoor HRAP and in a 14-L lab-scale HRAP,
77 respectively. Finally, (Hom-Diaz et al., 2017b) also reported a successful removal of
78 ciprofloxacin in a 1000-L outdoor HRAP during domestic wastewater treatment.

79 Despite these previous studies have consistently shown the potential of HRAPs for CEC
80 removal, the fate of these pollutants in innovative algal-bacterial photobioreactor

81 configurations has not been yet investigated. Hence, anoxic-aerobic algal-bacterial
82 photobioreactors have emerged as new configurations capable of treating low
83 carbon/nitrogen (C/N) wastewaters with a superior carbon and nutrient removal than
84 conventional HRAPs (Alcántara et al., 2015; de Godos et al., 2014; García et al., 2017). In
85 addition, anaerobic-anoxic-aerobic configurations based on photosynthetic oxygenation
86 have been proposed to foster phosphorous removal during wastewater treatments
87 (Metcalf et al., 2003).

88 In this context, the present work assessed for the first time the CEC removal performance
89 of two novel configurations consisting of anoxic-aerobic (phase A) and anaerobic-anoxic-
90 aerobic photobioreactors (phase B). The influence of parameters such as organic load,
91 HRT and external aeration on the removal of 5 pharmaceuticals and personal care
92 products (PPCPs) typically found in urban wastewaters (i.e., ibuprofen, naproxen, salicylic
93 acid, triclosan and propylparaben) was studied.

94

95 **2. Materials and methods**

96 **2.1 Experimental set-ups**

97 The experimentation was carried out in two phases. The first one, phase A, consisted of a
98 3.75-L enclosed anoxic bioreactor (AX) (15 cm long, 15 cm wide, 17 cm deep), an 11.25-L
99 open photobioreactor (HRAP) (30 cm long, 15 cm wide, 25 cm deep) and a 1-L conical
100 settler (Fig. 1). The 0.25/0.75 volume ratio of the AX and HRAP, and the depth of the

101 HRAP, were selected according to (Mosquera Corral, 2013) and (Sutherland et al., 2014),
102 respectively. Culture mixing in the anoxic tank and HRAP was provided by Eheim compact
103 300 immersion pumps (Spain) (one pump in the AX and two pumps in the HRAP). The
104 HRAP was exposed to a 12:12 h:h light:dark illumination regime at an average
105 photosynthetically active radiation (PAR) over the photobioreactor surface of 1314 ± 12
106 $\mu\text{mol m}^{-2} \text{s}^{-1}$ via high-intensity LED PCBs (Phillips SA, Spain). An internal liquid recirculation
107 (IR) from the HRAP to the AX supported the denitrification process and an external liquid
108 recirculation (ER) from the bottom of the settler to the AX supported algal-bacterial
109 biomass retention. The wastage of algal-bacterial biomass was conducted from the
110 bottom of the settler, to maintain a constant sludge retention time (SRT) (Fig. 1). Both the
111 SWW and treated effluent were stored in 20 L glass containers to avoid CECs adsorption.

112 In the second configuration, phase B, the set-up from phase A was modified by
113 implementing a 0.65-L enclosed anaerobic bioreactor (ANA) (8.7 cm long, 8.7 cm wide, 8.7
114 cm deep) before the AX. The ANA unit was directly fed with synthetic wastewater and the
115 ER from the settler, and discharged into AX by gravity. ANA was also mixed by an Eheim
116 compact 300 immersion pump (Spain) (Fig. 2).

117

118 **2.2 Algal-bacterial inoculum**

119 The anoxic-aerobic photobioreactor (phase A) was inoculated with a microalgal
120 consortium, collected from an outdoor pilot-scale HRAP treating centrate at the
121 Department of Chemical Engineering and Environmental Technology (University of

122 Valladolid, Spain) and with secondary activated sludge from Valladolid WWTP (operated
123 with a denitrification-nitrification configuration), in order to attain an initial total
124 suspended solids (TSS) concentration of 0.2 and 0.6 g TSS L⁻¹ of microalgae and activated
125 sludge, respectively.

126 On the other hand, the anaerobic-anoxic-aerobic photobioreactor (phase B) was
127 inoculated with a microalgae consortium collected from the anoxic-aerobic configuration
128 and 1 L of aerobic-anoxic sludge from Valladolid WWTP.

129

130 **2.3 Synthetic domestic wastewater**

131 Synthetic domestic wastewater (SWW) was prepared according to (Frutos et al., 2016) in
132 order to simulate a typical urban wastewater composition (Metcalf et al., 2003). The SWW
133 was composed of (g L⁻¹): casein peptone 0.16, meat extract 0.11, NH₂COH₂ 0.03, NaCl
134 0.007, CaCl₂·2H₂O 0.004, MgSO₄·7H₂O 0.002, CuCl₂·2H₂O 5·10⁻⁶, K₂HPO₄·3 H₂O 0.112,
135 C₆H₁₂O₆ 0.25 and NaHCO₃ 1.10. This resulted in concentrations of chemical oxygen
136 demand (COD) of 632±45 mg L⁻¹, total organic carbon (TOC) of 196±9 mg L⁻¹, inorganic
137 carbon (IC) of 195±12 mg L⁻¹, total nitrogen (TN) of 43±3 mg L⁻¹, N-NH₄⁺ of 24±3 mg L⁻¹, P-
138 PO₄⁻³ of 13.1±0.8 mg L⁻¹ and in a pH of 7.7±0.2. All reagents were purchased from
139 PANREAC (Barcelona, Spain) with a purity >98%. Ibuprofen, naproxen, salicylic acid,
140 triclosan and propylparaben were selected as model CECs based on their relevant
141 concentration levels and ubiquity in aquatic environments as well as their variable
142 degradability in conventional WWTPs (Hughes et al., 2013). An aliquot of a stock solution

143 containing the five CECs in methanol was daily added to the SWW to achieve a final
144 concentration of $8955 \pm 959 \text{ ng L}^{-1}$ of ibuprofen, $4177 \pm 128 \text{ ng L}^{-1}$ of naproxen, 62137 ± 1449
145 ng L^{-1} of salicylic acid, $537 \pm 11 \text{ ng L}^{-1}$ of triclosan and $408 \pm 31 \text{ ng L}^{-1}$ of propylparaben. This
146 represented a realistic scenario according to the typical values determined in different
147 wastewater treatment plants in Spain (Ortiz de García et al., 2013; Reyes-Contreras et al.,
148 2012; Reyes-Contreras et al., 2011). Additionally, these concentrations are not expected
149 to exert any biomass inhibitory effect. In fact, previous studies by the authors showed no
150 significant effect on HRAP performance at 2 mg L^{-1} of tetracycline, which represents more
151 than 20 times higher concentration of antibiotic than the combined concentration of all
152 the PPCPs assessed in the present study (de Godos et al., 2012). The CECs standards were
153 purchased from Sigma-Aldrich with a purity >99% and methanol was purchased from
154 PANREAC (purity >99%).

155

156 **2.4 Operational stages and sampling procedure**

157 In phase A, the bioreactors were initially filled with SWW, inoculated and operated at a
158 hydraulic retention time (HRT) of 4 d using a Watson Marlow 120 S pump (United
159 Kingdom) in order to acclimate the algal-bacterial consortium to the SWW. CECs were not
160 supplemented to the SWW during the acclimation period. The flow rates of the IR and ER
161 pumps (Watson Marlow 120 S 124 pump, United Kingdom, and Masterflex 7021-24,
162 United States, respectively) corresponded to 200% and 50% of the SWW flow rate,
163 respectively. The SRT of the system was fixed at 10 d. The initial 47 d acclimation period

164 was followed by a decrease in the HRT to 2 d and the supplementation of the SWW with
165 CECs. The flow rates of IR and ER were adjusted to the new SWW flow rate, while the SRT
166 was maintained at 10 d. Under these operational conditions, the influence of the COD
167 concentration (669 ± 6 mg L⁻¹ during stage A-I, 493 ± 11 mg L⁻¹ during stage A-II and 434 ± 11
168 mg L⁻¹ during stage A-III) on process performance was evaluated. Each operational stage
169 was maintained for 40 d (≈ 4 times the SRT) to achieve representative steady states, which
170 were kept for at least 10 days (thus allowing 4 replicate measurements). The system was
171 considered under steady state when the TOC, IC and TN removals, as well as the TSS
172 concentrations, varied less than 10% compared to the average values. The pH, dissolved
173 oxygen concentration (DO) and temperature were daily measured in the AX and HRAP.
174 The influent and effluent flow rates were also daily measured in order to determine the
175 evaporation rate, while the PAR was weekly monitored. Liquid samples of 50 mL were
176 drawn twice per week from the AX and HRAP to monitor the concentrations of TSS. The
177 influent and effluent concentrations of COD and CECs were measured at steady state. The
178 concentration of the H₂O₂ produced from photosynthetic microalgae activity in the HRAP
179 was also measured under steady state to determine its effect on CECs removal.

180 No acclimation period was necessary in phase B since the inoculum in the anaerobic-
181 anoxic-aerobic photobioreactor was obtained from phase A. The system was initiated at
182 an HRT of 4 d (Stage B-I). The flow rates of the IR and ER pumps corresponded to 200%
183 and 50% of the SWW flow rate, respectively. The SRT of the system was fixed at 10 d. The
184 SWW was supplemented with CECs. During stage B-II, the HRT was decreased to 3 d under
185 similar operating conditions to stage B-I (the flow rates of IR and ER were adjusted to the

186 new SWW flow rate, while the SRT was maintained at 10 d). Finally, 30 mL min⁻¹ of air
187 were bubbled into the HRAP during the night period in stage B-III in order to keep the
188 HRAP DO levels above 1.5 mg L⁻¹. Each operational stage was maintained for ≈4 times the
189 SRT in order to achieve representative steady states. The pH, dissolved oxygen
190 concentration (DO) and temperature were daily measured in the ANA, AX and HRAP. The
191 influent and effluent flow rates were also daily measured in order to determine the
192 evaporation rate, while the PAR was weekly monitored. Liquid samples of 50 mL were
193 drawn twice per week from the ANA, AX and HRAP to monitor the concentrations of TSS.
194 The influent and effluent concentrations of COD and CECs were measured under steady
195 state.

196

197 **2.5 Analytical methods**

198 The DO concentration and temperature were monitored with an OXI 330i oximeter (WTW,
199 Germany), while a pH meter Eutech Cyberscan pH 510 (Eutech instruments, The
200 Netherlands) was used for pH determination. The PAR was recorded with a LI- 250A light
201 meter (LI-COR Biosciences, Germany). The determination of TSS and COD concentration
202 was carried out according to standard methods (Eaton et al., 2005). The quantification,
203 identification and biometry measurements of microalgae population structure were
204 performed by microscopic examination (OLYMPUS IX70, USA). H₂O₂ was measured with a
205 Pierce Quantitative Peroxide Assay Kit (Thermo Scientific, USA).

206 CEs analyses were carried out according to (López-Serna et al., 2018). In brief, influent and
207 effluent wastewater samples (100 mL, in duplicate) were saturated with NaCl (400 g L⁻¹)
208 and pH adjusted to 3. Seventeen milliliters of the resulting solution were spiked with 100
209 ng of five isotopically labelled internal standards (i.e., ibuprofen-d3, propylparaben-d7,
210 salicylic acid-d4, naproxen-d3, triclosan-d3) and subsequently automatically analyzed by
211 online direct immersion solid phase microextraction (DI-SPME) on-fiber derivatization
212 followed by gas chromatography (GC) on a capillary HP-5MS column (30 m length,
213 0.25 mm i.d., 0.25 µm film thickness) coupled to mass spectrometry (MS) in selected ion
214 monitoring (SIM). Quantification based on peak areas was concurrently performed by
215 both matrix-matched and internal standard approaches. Method accuracy parameters are
216 shown as Supplementary data.

217

218 **3. Results and discussion**

219 The evaporation rate in the HRAP remained approx. constant at 15 L m⁻² d⁻¹ regardless of
220 the operational stage in phase A (Table 1). During phase B, evaporation rates accounted
221 for 13-16 L m⁻² d⁻¹ in stages B-I and B-II, respectively, and increased to 20 L m⁻² d⁻¹ in stage
222 B-III (Table 2). These high evaporation rates compared to the water losses in industrial
223 scale HRAP (≈3-8 L m⁻² d⁻¹) were caused by the high turbulence induced by an
224 overdimensioned immersion pump in this lab scale HRAP (Guieysse et al., 2013). This
225 phenomenon was aggravated in stage B-III, where additional aeration was supplied during

226 the night period. In this context, water losses resulted in 7-16% higher CECs
227 concentrations in the effluent along the whole experimentation.

228 The organic nitrogen present in the SWW as protein (around 19 mg L^{-1}) was expected to
229 undergo ammonification in the anaerobic tank and subsequent nitrification in the HRAP
230 tank. In the absence of strong natural buffers, the pH was expected to drop as a result of
231 NH_4^+ oxidation to nitrate. However, photosynthetic activity increased the pH in the HRAP
232 compared to the anaerobic and anoxic tanks (Table 1 and Table 2). Surprisingly, lower
233 organic loads mediated lower pHs in the HRAP during phase A, which ultimately resulted
234 in similar pHs during stage A-III in both bioreactors (≈ 8.2 and 8.4 in AX and HRAP,
235 respectively). In phase B, the lowest pH values were observed in ANA (≈ 7.8), which was
236 attributed to the typical acidification of anaerobic processes. The highest values were
237 again observed in the HRAP (≈ 9.8), which were higher than in the HRAP during phase A
238 and considered a proxy of a more intense photosynthetic activity. In any case, pH values
239 remained within the optimum range to support microbial activity (Posadas et al., 2015).

240 The DO concentrations in AX remained lower than $\approx 0.3 \text{ mg L}^{-1}$ (Table 1) during phase A
241 due to its enclosed nature and absence of photosynthetic activity. These DO levels were
242 suitable to support denitrification, which typically requires DO concentrations lower than
243 1 mg L^{-1} (Metcalf et al., 2003). DO concentration in the HRAP increased at decreasing COD
244 loads in phase A due to the reduced heterotrophic oxygen demand to oxidize the organic
245 matter present in the SWW. During phase B, DO concentrations remained at $\approx 0 \text{ mg O}_2 \text{ L}^{-1}$
246 and below $1 \text{ mg O}_2 \text{ L}^{-1}$ in ANA and AX, respectively (Table 2). DO in the HRAP remained

247 around 13 mg O₂ L⁻¹ in stage B-I, but dropped to 5 mg O₂ L⁻¹ during stage B-II due to the
248 increase in the heterotrophic and nitrifying oxygen demand mediated by the decrease in
249 HRT. This severely limited the nitrification processes during stage B-II, which was
250 recovered in stages B-III by bubbling air during the night period.

251 The temperatures in the cultivation broth of the HRAP were usually the highest in both
252 phases as a result of the heat irradiated by the LEDs (Table 1 and Table2). In phase B, the
253 temperatures in ANA remained above those recorded in AX (Table 2). Regardless, the
254 observed temperatures in all the bioreactors (23-30 C) were suitable to support an
255 optimum biological wastewater treatment regardless of the stage. In this context,
256 Removal efficiencies (REs) of ibuprofen, naproxen and salicylic acid have been reported to
257 increase by ~ 10-20% when temperature increased from 12 C to 26 C (Hijosa-Valsero et al.,
258 2010). In our particular study, the influence of temperature on CECs removal was likely
259 negligible due to the fact that the highest difference in temperature per unit along each
260 phase was 5 C (Table 1 and Table 2).

261 The microalgae population (percentage of cells) during phase A was mainly composed of
262 *Chlorella vulgaris*, with abundances of 55% and 48% in A-I and A-II, respectively. However,
263 *Phormidium sp.*, which was absent during A-I and represented only 27% of microalgae
264 cells in A-II, increased up to 39% during A-III, representing the most popular species
265 followed by *Chlorella vulgaris*, which dropped to 28%. During phase B, *Chlorella vulgaris*
266 was also the most abundant species with abundances of 65 and 47% in B-I and B-II,
267 respectively, followed by *Scenedesmus acuminatus* (with abundances of 24 and 38% in

268 stage B-I and B-II, respectively). Interestingly, the addition of external aeration modified
269 the microalgae population structure. Hence, *Pseudonabaena acicularis* and *Scenedesmus*
270 *acutus* accounted for 67 and 16% of the total microalgae population during stage B-III,
271 respectively, while *Chlorella vulgaris* dropped to levels of 8% during this stage. At this
272 point it should be highlighted that the active internal and external recirculation (2.5 times
273 the SWW flowrate) resulted in a complete mixing of the cultivation broth and therefore a
274 similar microalgae population structure in the three bioreactor units.

275 These novel configurations and operational conditions supported effective COD removals
276 of 84±0%, 89±1%, 86±1%, 90±1%, 94±1% and 94±0%, which resulted in COD effluent
277 concentrations of 116±4 mg L⁻¹, 61±5 mg L⁻¹, 67±7 mg L⁻¹, 70±10 mg L⁻¹, 45±4 mg L⁻¹ and
278 46±1 mg L⁻¹ during stages A-I, A-II, A-III, B-I, B-II and B-III, respectively. In this regard, the
279 treated effluent complied with the limits of COD concentration (≤125 mg L⁻¹) required by
280 the EU Water Framework Directive for wastewater disposal into the environment
281 (Directive 2000/60/EC) (European Commission, 2000) (European Commission, 2000).

282 The highest TSS concentrations were recorded in the HRAP (≈ 0.7-1.4 g L⁻¹) (Table 1 and
283 Table 2), which was likely mediated by the superior carbon and nutrient removal
284 mediated by algal activity in the photobioreactor (Posadas et al., 2013). In addition,
285 effluent TSS concentrations were always within the discharge limit for wastewater during
286 phases A and B regardless of the operational conditions.

287 Finally, H₂O₂, a byproduct from algal photosynthetic activity, was not detected along the
288 whole experimentation, which ruled out a potential contribution of chemical oxidation to

289 CECs removal in the HRAP (Fukuzumi, 2016). Likewise, UV photodegradation was not
290 considered as a potential mechanism of CECs' removal in this research based on the fact
291 that the wavelength of the LEDs here used only comprised the range 400-700 nm.
292 Similarly, volatilization was not likely a significant mechanism of CEC removal based on the
293 fact that the vapor pressures of the 5 target CECs remained below 0.15 Pa at the range of
294 temperatures prevailing in the experimental set-up along the experiment.

295

296 **3.1 Ibuprofen removal**

297 In the anoxic-aerobic photobioreactor, Ibuprofen REs of 26±13%, 76±2% and 91±1% were
298 recorded in stages A-I, A-II and A-III, respectively (Fig. 3). The concentration of ibuprofen
299 in the effluent at the highest RE was $\approx 894 \text{ ng L}^{-1}$, which would correspond to $\approx 834 \text{ ng L}^{-1}$ in
300 absence of water evaporation. The elimination of ibuprofen in stage A-III was similar to
301 that reported by (Hom-Diaz et al., 2017a; Matamoros et al., 2015), who always detected
302 ibuprofen removals >86% and concentrations < 900 ng L^{-1} in the effluent of two 470-L
303 outdoor single-stage HRAPs during the treatment of urban wastewater regardless of the
304 season and HRT. It should be noticed that in those studies, solar UV-mediated
305 photodegradation was expected to be an important elimination mechanism. In our
306 particular study, lower COD loads were correlated to higher ibuprofen REs, likely due to
307 the increase in DO in the cultivation broth of the HRAP, which triggered the removal of
308 this CEC by biological oxidation (Matamoros et al., 2016). An enhancement in the
309 nitrification activity was also observed in stages A-II and A-III mediated by the higher DO.

310 This could have also contributed to the improvement in the ibuprofen removal as
311 previously reported by (Fernandez-Fontaina et al., 2012) in activated sludge systems.

312 In the anaerobic-anoxic-aerobic photobioreactor, Ibuprofen was removed at higher
313 efficiencies than in phase A. Indeed, REs of $94\pm 1\%$, $93\pm 3\%$ and $81\pm 0\%$ were recorded in
314 stages B-I, B-II and B-III, respectively (Fig. 3). Hence, no significant influence of HRT and
315 the DO was observed in the anaerobic-anoxic-aerobic photobioreactor. These results
316 confirmed that this novel configuration did not impact the good CEC removal performance
317 observed in single-stage HRAPs by (Hom-Diaz et al., 2017a; Matamoros et al., 2015),
318 where REs above 86% were recorded at a HRT of 4 d.

319 Ibuprofen removal by biomass sorption could be considered negligible in both phases at
320 the operational pH in ANA, AX and HRAP due to its negative charge (ibuprofen $pK_a\approx 4.41$)
321 and the electrochemical negative charge of the microalgae cells walls (Matamoros et al.,
322 2015; Matamoros et al., 2016). Hence, biodegradation was likely the main mechanism
323 governing ibuprofen removal in this study. This was in agreement with the study
324 conducted by (Matamoros et al., 2016), who reported an increase of up to 40% in
325 ibuprofen removal due to the synergetic interaction between algae and bacteria.

326

327 **3.2 Naproxen removal**

328 In the anoxic-aerobic photobioreactor, naproxen removal was only effective during stage
329 A-III at $28\pm 7\%$, which resulted in concentrations in the effluent of $\approx 3239 \text{ ng L}^{-1}$ ($\approx 3022 \text{ ng L}^{-1}$

330 ¹ without evaporation) (Fig. 4). In fact, naproxen was the CEC that exhibited the lowest RE
331 of all studied ones. These naproxen REs were in accordance with the 33% reported in a
332 waste stabilization pond during urban wastewater treatment (Hijosa-Valsero et al., 2010).
333 Even lower elimination efficiencies (10%) were observed by (Hom-Diaz et al., 2017a) when
334 toilet wastewater was treated in a single-stage pilot-scale HRAP operated at a HRT of 8 d.
335 In contrast, (Matamoros et al., 2015) recorded naproxen REs of 60-90% during urban
336 wastewater treatment in two 470-L outdoor single-stage HRAPs, where in contrast to our
337 study, solar UV-mediated photodegradation was likely a key removal mechanism. In our
338 particular study, the lower COD loads and higher DO concentration in stage A-III could
339 have supported a significant naproxen removal by biological oxidation. In this sense, the
340 enhanced nitrification activity occurring under these operational conditions could have
341 also influenced naproxen removal (Fernandez-Fontaina et al., 2012). Additionally,
342 microalgae inhibition at naproxen concentrations higher than 100 ppm has been reported
343 (Fernandez-Fontaina et al., 2012). In this context, and despite the lower concentrations
344 here tested ($\leq 4.2 \cdot 10^{-3}$ ppm), the absence of naproxen removal observed during the first
345 two stages in phase A might have been due to microbial acclimation to this pollutant.

346 Overall, the anaerobic-anoxic-aerobic photobioreactor was more efficient at removing
347 naproxen than the anoxic-aerobic photobioreactor. Hence, REs of $44 \pm 11\%$, $24 \pm 1\%$ and
348 $52 \pm 7\%$ were recorded in stage B-I, B-II and B-III, respectively (Fig. 4). Thus, biodegradation
349 could be pointed out as a major elimination mechanism again as a result of the enhanced
350 photosynthetic activity and longer HRT during phase B. Those removal efficiencies were
351 similar to the ones reported by (Matamoros et al., 2015) at a HRT of 4 d in a single-stage

352 HRAP during cold season ($48\pm 5\%$). Interestingly, a reduction in naproxen removal
353 efficiency was observed in stage B-II when DO levels in HRAP decreased below 1.5 mg L^{-1} ,
354 which suggests the key role of biological oxidation on the removal of this anti-
355 inflammatory drug. Finally, it should be highlighted that CEC sorption into biomass could
356 be discarded as a removal mechanism in the systems due to its low pKa (≈ 4.84) compared
357 to the pH in the bioreactors.

358

359 **3.3 Salicylic acid**

360 Steady state salicylic acid REs during the operation of the anoxic-aerobic photobioreactor
361 accounted for $63\pm 1\%$, $83\pm 5\%$ and $74\pm 8\%$ in stages A-I, A-II and A-III, respectively (Fig. 5).
362 The minimum salicylic acid concentration in the effluent was $\approx 11691 \text{ ng L}^{-1}$ during stage A-
363 II ($\approx 10756 \text{ ng L}^{-1}$ without water evaporation). The moderate increase in RE from stage A-I
364 to stages A-II and A-III showed the low influence of COD load on salicylic acid removal. The
365 REs herein recorded were lower than the reported values of 93% and 98% by (Escapa et
366 al., 2017) during the evaluation of salicylic acid removal at 25 mg L^{-1} and at 250 mg L^{-1} ,
367 respectively, by *Chlorella sorokiniana* in a 250 mL bubbling column photobioreactor
368 illuminated at $370 \mu\text{mol m}^{-2} \text{ s}^{-1}$ at 12:12 h with 8 fluorescent lamps (58 W, 2150 lumen,
369 Philips, France). These authors concluded that *C. sorokiniana* was able to use salicylic acid
370 as an additional carbon source. Differences in results could be attributed to the high
371 concentrations tested there, in comparison to the realistic ppb levels assessed in our
372 study.

373 On the other hand, salicylic acid REs in the anaerobic-anoxic-aerobic photobioreactor
374 were generally similar to those recorded in the anoxic-aerobic system (except in stage B-
375 II). In particular, REs of $97\pm 2\%$, $34\pm 25\%$ and $75\pm 7\%$ were achieved in stages B-I, B-II and B-
376 III, respectively (Fig. 5). These high elimination efficiencies were similar to the ones
377 reported by (Escapa et al., 2017; Hom-Diaz et al., 2017a) in the studies described above,
378 despite no UV photodegradation contribution occurred in the present research. The
379 occurrence of episodes at DO close to 0 were frequent during stage B-II and could explain
380 the poor removal of this CEC during that stage. This would lead to confirm biodegradation
381 as a major salicylic acid removal mechanism. Similarly to the rationale described for
382 naproxen and ibuprofen, sorption was not considered a relevant mechanism based on the
383 low pKa (≈ 3.01) of this CEC, which is far too low from the pH values observed in the
384 bioreactors along the whole experimentation.

385

386 **3.4 Triclosan**

387 Triclosan REs of $68\pm 3\%$, $85\pm 0\%$ and $83\pm 0\%$ were recorded in the anoxic-aerobic
388 photobioreactor in stages A-I, A-II and A-III, respectively (Fig. 6). Thus, the minimum
389 concentration of triclosan in the effluent was $\approx 89 \text{ ng L}^{-1}$ ($\approx 82 \text{ ng L}^{-1}$ without water losses).
390 Similarly to the pattern recorded for salicylic acid, comparable degradation efficiencies of
391 triclosan were recorded regardless of the COD load applied. These high REs agreed with
392 those reported by (Matamoros et al., 2015), who classified triclosan as a moderate-highly

393 degradable CEC (REs of 60-90%) during urban wastewater treatment in two 470-L outdoor
394 HRAPs.

395 The anaerobic-anoxic-aerobic photobioreactor supported higher efficiencies than those
396 achieved in the anoxic-aerobic photoreactor. In particular, triclosan REs of $73\pm 0\%$, $100\pm 0\%$
397 and $100\pm 0\%$ were recorded in stage B-I, B-II, B-III and B-IV, respectively (Fig. 6). This
398 showed that the enhanced denitrification processes achieved during phase B, as well as
399 the higher HRT, contributed positively to triclosan elimination. Thus, this novel
400 photobioreactor configuration turned out to be more advantageous than single-stage
401 HRAPs for the elimination of triclosan (Matamoros et al., 2015).

402 The high temperatures prevailing in our experimental set-ups in phase A and B likely
403 supported an effective triclosan removal by biodegradation (Hoque et al., 2014). In fact,
404 (Wang et al., 2018) recently concluded that cellular uptake and biotransformation are
405 major removal mechanisms of triclosan in microalgae cultures at a pH of 7.5, which
406 suggests the key role of enzymatic triclosan degradation in our photobioreactors.
407 However, triclosan removal by sorption into biomass should be also considered based on
408 its pKa (≈ 7.80), which was close to the above-mentioned range of pHs in the ANA and AX
409 units (Matamoros et al., 2015).

410

411 **3.5 Propylparaben**

412 Propylparaben REs of $87\pm 0\%$, $81\pm 17\%$ and $85\pm 15\%$ were recorded in stages A-I, A-II and A-
413 III, respectively, in the anoxic-aerobic photobioreactor (Fig. 7). These high REs resulted in
414 propylparaben concentrations in the effluent of $\approx 55 \text{ ng L}^{-1}$ ($\approx 52 \text{ ng L}^{-1}$ without water
415 losses). This research was the first time propylparaben was assessed under microalgae-
416 based water treatment. Nonetheless, these REs were similar to the eliminations reported
417 in conventional activated sludge WWTPs ($>90\%$) (Haman et al., 2015). Interestingly,
418 propylparaben removal was not dependent on COD loads.

419 The anaerobic-anoxic-aerobic photobioreactor supported steady state propylparaben REs
420 of $73\pm 0\%$, $100\pm 0\%$ and $100\pm 0\%$ during stage B-I, B-II and B-III, respectively) (Fig. 7).

421 The degradation profiles recorded in phase A and B were almost identical to the ones
422 observed for triclosan. Indeed, propylparaben exhibits a high pKa (≈ 8.23) too, similar to
423 the pH value of the cultivation in ANA, AX and HRAP during most of both experiments,
424 which likely supported a significant contribution of sorption into biomass to the removal
425 of propylparaben as well. Nevertheless, there is also consistent evidence in literature that
426 supports the high biodegradability of parabens ($>90\%$), which suggests that
427 biodegradation might have played also a major role on propylparaben fate in the
428 photobioreactors (González-Mariño et al., 2011).

429

430 **4. Conclusions**

431 To the best of our knowledge, this research constitutes the first time the removal of CECs
432 from domestic wastewater was evaluated in two novel anoxic-aerobic and anaerobic-
433 anoxic-aerobic photobioreactor configurations. Overall, the set-up including the anaerobic
434 process exhibited higher removals of the five PPCPs than the anoxic-aerobic
435 photobioreactor. This superior performance could have been mediated by the higher HRT,
436 and enhanced denitrification processes and photosynthetic oxygenation, which supported
437 biodegradation as a major mechanism in the elimination of the five CECs. In contrast,
438 volatilization and photodegradation phenomena were discarded due to the low vapor
439 pressure of the contaminants and the use of visible LED lamps, respectively. On other
440 hand, the high pKa of triclosan and propylparaben could have promoted sorption onto the
441 biomass as an extra via of elimination for these two CECs, which could explain the higher
442 REs observed for triclosan and propylparaben in comparison to the other more polar CECs.
443 Furthermore, sorption is not expected to depend on the COD or DO levels and could have
444 supported their efficient REs during stages A-I, A-II and B-II despite the low DO. Overall,
445 despite these novel photobioreactor configurations have not been specifically designed to
446 eliminate CECs but to enhance nitrogen removal, CEC-REs were improved with respect to
447 single-stage HRAPs.

448

449 **ACKNOWLEDGEMENTS**

450 This research was supported by the FEDER program, the regional government of Castilla y
451 León (UIC71, CLU 2017-09) and the Spanish Ministry of Science, Innovation and

452 Universities (RED NOVEDAR and CTQ2017-84006-C3-1-R projects). Rebeca López Serna
453 acknowledges her grant Juan de la Cierva Incorporación JCI -2015-23304 to the Spanish
454 Ministry of Science, Innovation and Universities. Araceli Crespo and Jonatan Prieto are
455 gratefully acknowledged for their technical support.

456

457 REFERENCES

458 Alan MV, Barber LB, Gray JL, Lopez EM, Woodling JD, Norris DO. Reproductive disruption
459 in fish downstream from an estrogenic wastewater effluent. *Environmental*
460 *Science and Technology* 2008; 42: 3407-3414.

461 Alcántara C, Domínguez JM, García D, Blanco S, Pérez R, García-Encina PA, et al. Evaluation
462 of wastewater treatment in a novel anoxic-aerobic algal-bacterial photobioreactor
463 with biomass recycling through carbon and nitrogen mass balances. *Bioresource*
464 *Technology* 2015; 191: 173-186.

465 de Godos I, Muñoz R, Guieysse B. Tetracycline removal during wastewater treatment in
466 high-rate algal ponds. *Journal of Hazardous Materials* 2012; 229-230: 446-449.

467 de Godos I, Vargas VA, Guzmán HO, Soto R, García B, García PA, et al. Assessing carbon
468 and nitrogen removal in a novel anoxic-aerobic cyanobacterial-bacterial
469 photobioreactor configuration with enhanced biomass sedimentation. *Water*
470 *Research* 2014; 61: 77-85.

471 Eaton AD, Clesceri LS, Rice EW, Greenberg AE, M. Franson AH. APHA: standard methods
472 for the examination of water and wastewater. Centen Ed APHA, AWWA, WEF
473 2005.

474 Escapa C, Coimbra RN, Paniagua S, García AI, Otero M. Paracetamol and salicylic acid
475 removal from contaminated water by microalgae. Journal of Environmental
476 Management 2017; 203: 799-806.

477 European Commission. Directive 2000/60/EC of the european parliament and of the
478 council of 23 October 2000 establishing a framework for Community action in the
479 field of water policy. In: Communities TCotE, editor, 2000.

480 European Commission. Directive 2013/39/EU of the european parliament and of the
481 council of 12 August 2013 amending Directives 2000/60/EC and 2008/105/EC as
482 regards priority substances in the field of water policy 2013.

483 Fernandez-Fontaina E, Omil F, Lema JM, Carballa M. Influence of nitrifying conditions on
484 the biodegradation and sorption of emerging micropollutants. Water Research
485 2012; 46: 5434-5444.

486 Frutos OD, Quijano G, Pérez R, Muñoz R. Simultaneous biological nitrous oxide abatement
487 and wastewater treatment in a denitrifying off-gas bioscrubber. Chemical
488 Engineering Journal 2016; 288: 28-37.

489 Fukuzumi S. Artificial photosynthesis for production of hydrogen peroxide and its fuel
490 cells. Biochimica et Biophysica Acta - Bioenergetics 2016; 1857: 604-611.

491 García D, Alcántara C, Blanco S, Pérez R, Bolado S, Muñoz R. Enhanced carbon, nitrogen
492 and phosphorus removal from domestic wastewater in a novel anoxic-aerobic
493 photobioreactor coupled with biogas upgrading. *Chemical Engineering Journal*
494 2017; 313: 424-434.

495 González-Mariño I, Quintana JB, Rodríguez I, Cela R. Evaluation of the occurrence and
496 biodegradation of parabens and halogenated by-products in wastewater by
497 accurate-mass liquid chromatography-quadrupole-time-of-flight-mass
498 spectrometry (LC-QTOF-MS). *Water Research* 2011; 45: 6770-6780.

499 Guieysse B, Béchet Q, Shilton A. Variability and uncertainty in water demand and water
500 footprint assessments of fresh algae cultivation based on case studies from five
501 climatic regions. *Bioresource Technology* 2013; 128: 317-323.

502 Haman C, Dauchy X, Rosin C, Munoz JF. Occurrence, fate and behavior of parabens in
503 aquatic environments: A review. *Water Research* 2015; 68: 1-11.

504 Hijosa-Valsero M, Matamoros V, Martín-Villacorta J, Bécares E, Bayona JM. Assessment of
505 full-scale natural systems for the removal of PPCPs from wastewater in small
506 communities. *Water Research* 2010; 44: 1429-1439.

507 Hom-Díaz A, Jaén-Gil A, Bello-Laserna I, Rodríguez-Mozaz S, Vicent T, Barceló D, et al.
508 Performance of a microalgal photobioreactor treating toilet wastewater:
509 Pharmaceutically active compound removal and biomass harvesting. *Science of*
510 *The Total Environment* 2017a; 592: 1-11.

511 Hom-Diaz A, Norvill ZN, Blázquez P, Vicent T, Guieysse B. Ciprofloxacin removal during
512 secondary domestic wastewater treatment in high rate algal ponds. *Chemosphere*
513 2017b; 180: 33-41.

514 Hoque ME, Cloutier F, Arcieri C, McInnes M, Sultana T, Murray C, et al. Removal of
515 selected pharmaceuticals, personal care products and artificial sweetener in an
516 aerated sewage lagoon. *Science of the Total Environment* 2014; 487: 801-812.

517 Hughes SR, Kay P, Brown LE. Global synthesis and critical evaluation of pharmaceutical
518 data sets collected from river systems. *Environmental Science and Technology*
519 2013; 47: 661-677.

520 López-Serna R, Marín-de-Jesús D, Irusta-Mata R, García-Encina PA, Lebrero R, Fdez-
521 Polanco M, et al. Multiresidue analytical method for pharmaceuticals and personal
522 care products in sewage and sewage sludge by online direct immersion SPME on-
523 fiber derivatization – GCMS. *Talanta* 2018; 186: 506-512.

524 Matamoros V, Gutiérrez R, Ferrer I, García J, Bayona JM. Capability of microalgae-based
525 wastewater treatment systems to remove emerging organic contaminants: A pilot-
526 scale study. *Journal of Hazardous Materials* 2015; 288: 34-42.

527 Matamoros V, Uggetti E, García J, Bayona JM. Assessment of the mechanisms involved in
528 the removal of emerging contaminants by microalgae from wastewater: A
529 laboratory scale study. *Journal of Hazardous Materials* 2016; 301: 197-205.

530 Metcalf, Eddy I, Tchobanoglous G, Burton F, Stensel HD. Wastewater Engineering:
531 Treatment and Reuse: McGraw-Hill Education, 2003.

532 Mosquera Corral A. Tecnologías Avanzadas para el tratamiento de aguas residuales.
533 Novedar-Consolider, Santiago de Compostela 2013.

534 Norvill ZN, Shilton A, Guieysse B. Emerging contaminant degradation and removal in algal
535 wastewater treatment ponds: Identifying the research gaps. Journal of Hazardous
536 Materials 2016; 313: 291-309.

537 Norvill ZN, Toledo-Cervantes A, Blanco S, Shilton A, Guieysse B, Muñoz R.
538 Photodegradation and sorption govern tetracycline removal during wastewater
539 treatment in algal ponds. Bioresource Technology 2017; 232: 35-43.

540 Orlando EF, Ellestad LE. Sources, concentrations, and exposure effects of environmental
541 gestagens on fish and other aquatic wildlife, with an emphasis on reproduction.
542 General and Comparative Endocrinology 2014; 203: 241-249.

543 Ortiz de García S, Pinto Pinto G, García Encina P, Irusta Mata R. Consumption and
544 occurrence of pharmaceutical and personal care products in the aquatic
545 environment in Spain. Science of the Total Environment 2013; 444: 451-465.

546 Posadas E, García-Encina PA, Soltau A, Domínguez A, Díaz I, Muñoz R. Carbon and nutrient
547 removal from centrates and domestic wastewater using algal-bacterial biofilm
548 bioreactors. Bioresource Technology 2013; 139: 50-58.

549 Posadas E, Morales MDM, Gomez C, Ación FG, Muñoz R. Influence of pH and
550 CO₂ source on the performance of microalgae-based secondary
551 domestic wastewater treatment in outdoors pilot raceways. *Chemical Engineering*
552 *Journal* 2015; 265: 239-248.

553 Reyes-Contreras C, Hijosa-Valsero M, Sidrach-Cardona R, Bayona JM, Bécares E. Temporal
554 evolution in PPCP removal from urban wastewater by constructed wetlands of
555 different configuration: A medium-term study. *Chemosphere* 2012; 88: 161-167.

556 Reyes-Contreras C, Matamoros V, Ruiz I, Soto M, Bayona JM. Evaluation of PPCPs removal
557 in a combined anaerobic digester-constructed wetland pilot plant treating urban
558 wastewater. *Chemosphere* 2011; 84: 1200-1207.

559 Rivera-Utrilla J, Sánchez-Polo M, Ferro-García MÁ, Prados-Joya G, Ocampo-Pérez R.
560 Pharmaceuticals as emerging contaminants and their removal from water. A
561 review. *Chemosphere* 2013; 93: 1268-1287.

562 Sutherland DL, Turnbull MH, Craggs RJ. Increased pond depth improves algal productivity
563 and nutrient removal in wastewater treatment high rate algal ponds. *Water*
564 *Research* 2014; 53: 271-281.

565 Wang S, Poon K, Cai Z. Removal and metabolism of triclosan by three different microalgal
566 species in aquatic environment. *Journal of Hazardous Materials* 2018; 342: 643-
567 650.

568

Table 1. Data of process performance during the removal of ECs from synthetic urban wastewater in the anoxic (AX) and aerobic (HRAP) bioreactors during phase A under steady state.

	STAGE A-I HRT=2 d COD=669±6 mg O₂ L⁻¹	STAGE A-II HRT=2 d COD=493±11 mg O₂ L⁻¹	STAGE A-III HRT=2 d COD=434±11 mg O₂ L⁻¹
Evaporation rate (L m⁻² d⁻¹)	14±1	15±2	15±2
pH_{AX}	8.2±0.2	8.1±0.1	8.2±0.2
pH_{HRAP}	9.0±0.1	8.7±0.1	8.4±0.3
DO_{AX} (mg O₂ L⁻¹)	0.1±0.1	0.2±0.1	0.3±0.2
DO_{HRAP} (mg O₂ L⁻¹)	0.4±0.1	3.4±2.6	4.7±3.6
T_{AX} (°C)	24±1	26±2	27±1
T_{HRAP} (°C)	26±0	28±2	29±1
TSS_{AX} (g L⁻¹)	0.7±0.1	0.5±0.1	0.6±0.1
TSS_{HRAP} (g L⁻¹)	1.0±0.1	0.7±0.0	1.0±0.1

Table 2. Data of process performance during the removal of ECs from synthetic urban wastewater in the anaerobic (ANA), anoxic (AX) and aerobic (HRAP) bioreactors during phase B under steady state.

	STAGE B-I HRT=4 d COD=669±6 mg O₂ L⁻¹	STAGE B-II HRT=3 d COD=669±6 mg O₂ L⁻¹	STAGE B-III HRT=3 d COD=669±6 mg O₂ L⁻¹
Evaporation rate (L m⁻² d⁻¹)	13±1	16±3	20 ±0
pH_{ANA}	8.6±0.1	7.4±0.2	7.7±0.2
pH_{AX}	9.0±0.2	8.1±0.1	8.1±0.1
pH_{HRAP}	9.8±0.1	8.8±0.3	8.7±0.2
DO_{ANA} (mg O₂ L⁻¹)	0.0±0.0	0.0±0.0	0.0±0.1
DO_{AX} (mg O₂ L⁻¹)	0.9±0.7	0.2±0.7	0.3±0.6
DO_{HRAP} (mg O₂ L⁻¹)	13.0±6.0	5.0±5.4	10.4±6.3
T_{ANA} (C)	27	28	28
T_{AX} (C)	25	27	29
T_{HRAP} (C)	29	29	30
TSS_{ANA} (g L⁻¹)	0.7±0.2	1.2±0.1	1.5±0.1
TSS_{AX} (g L⁻¹)	0.6±0.2	0.7±0.1	1.2±0.2
TSS_{HRAP} (g L⁻¹)	1.0±0.2	1.2±0.0	1.4±0.4

Figure 1. Schematic of the anoxic-aerobic photobioreactor.

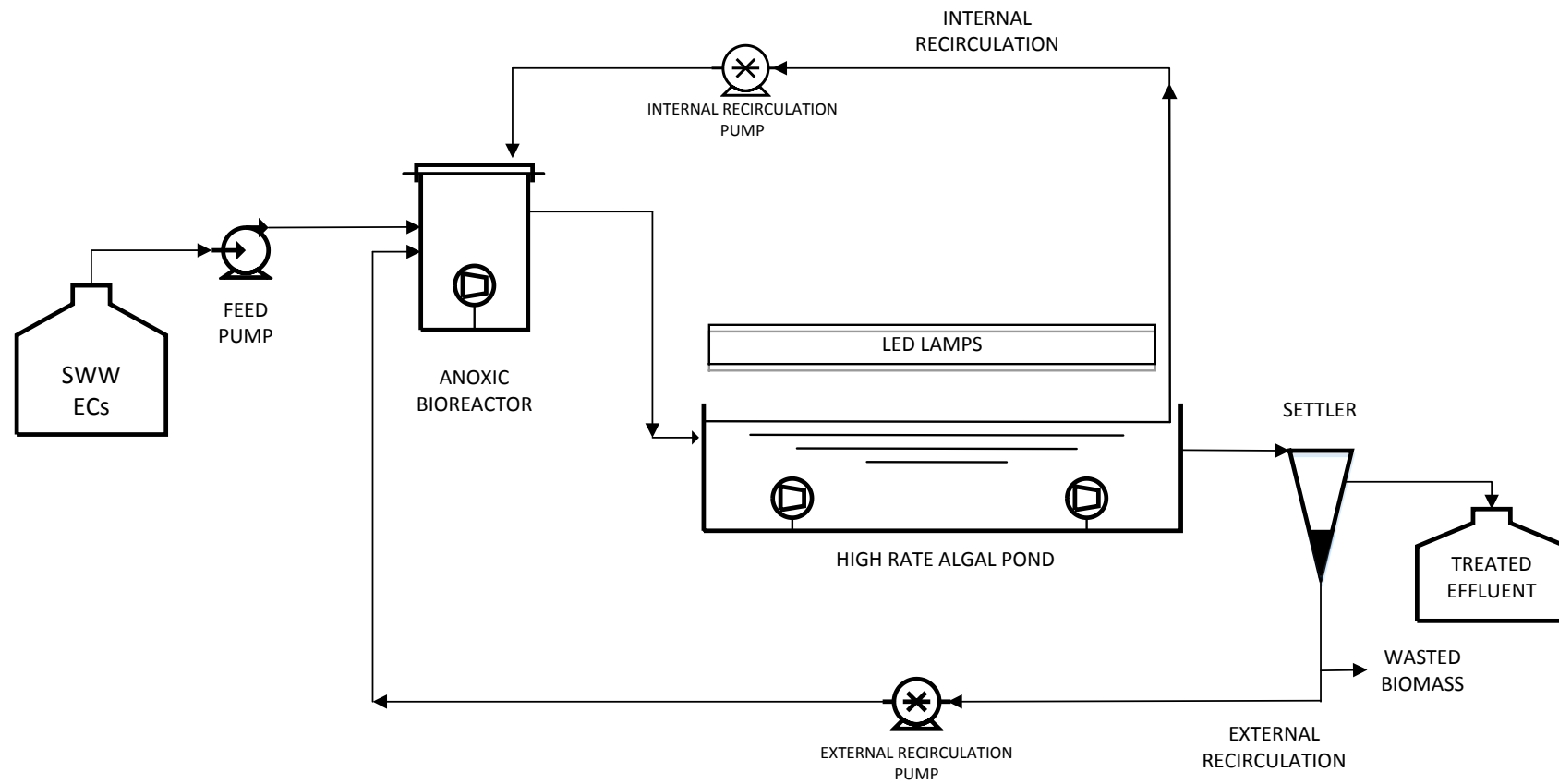


Figure 2. Schematic of the anaerobic-anoxic-aerobic photobioreactor.

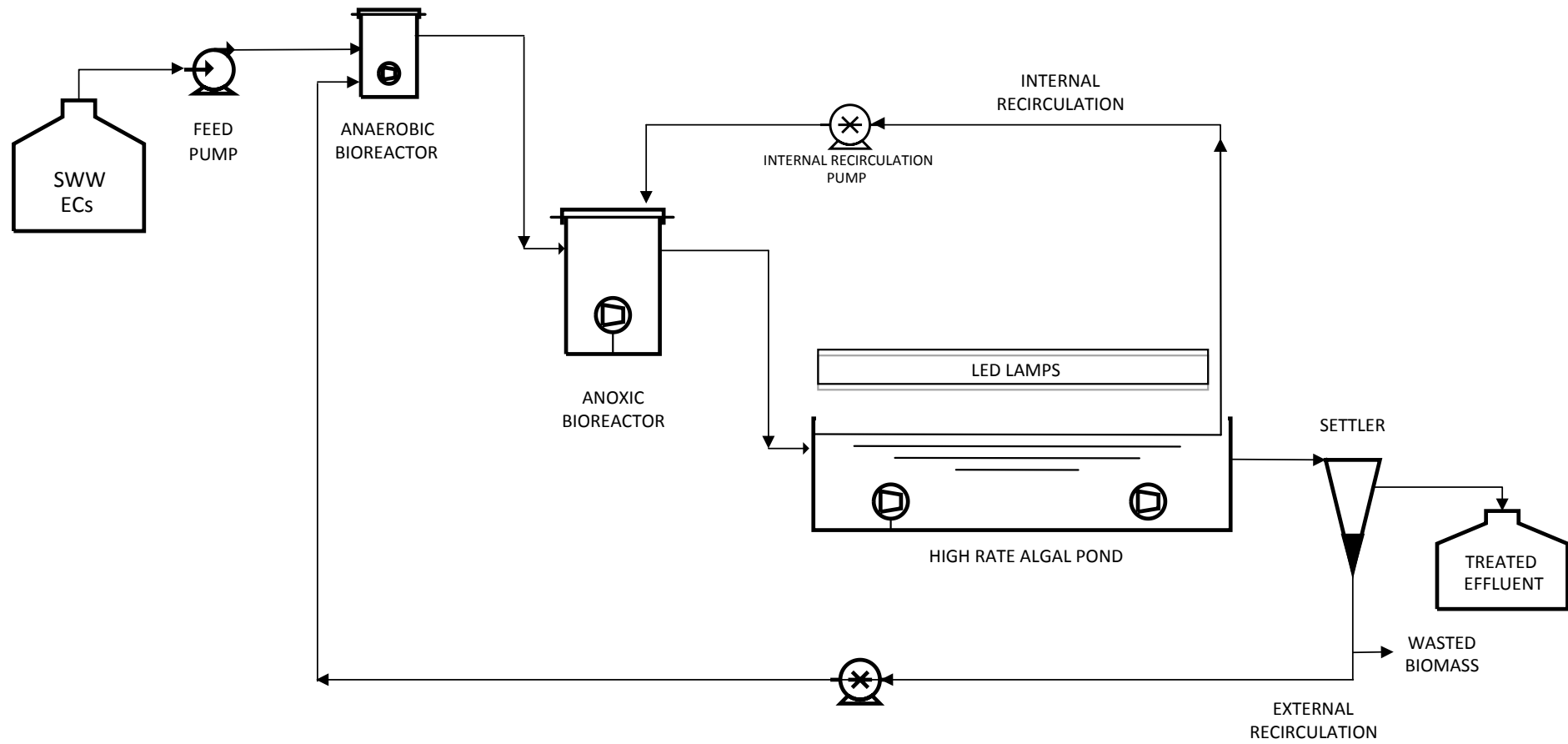
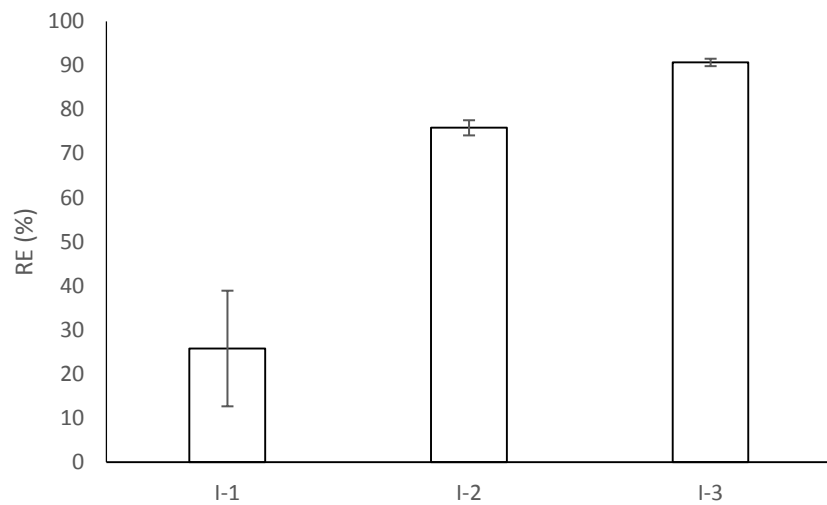


Figure 3. Steady state removal efficiencies of ibuprofen during phase A (a) and phase B (b). Vertical bar correspond to standard deviations from replicates.

a)



b)

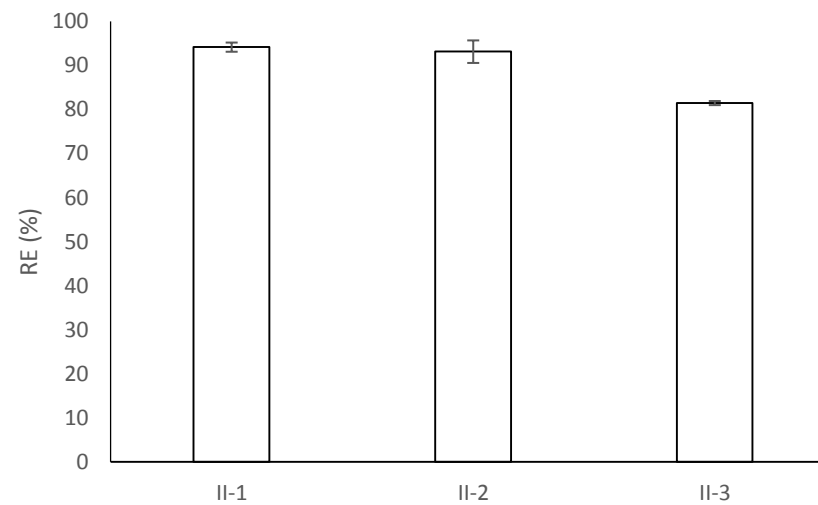
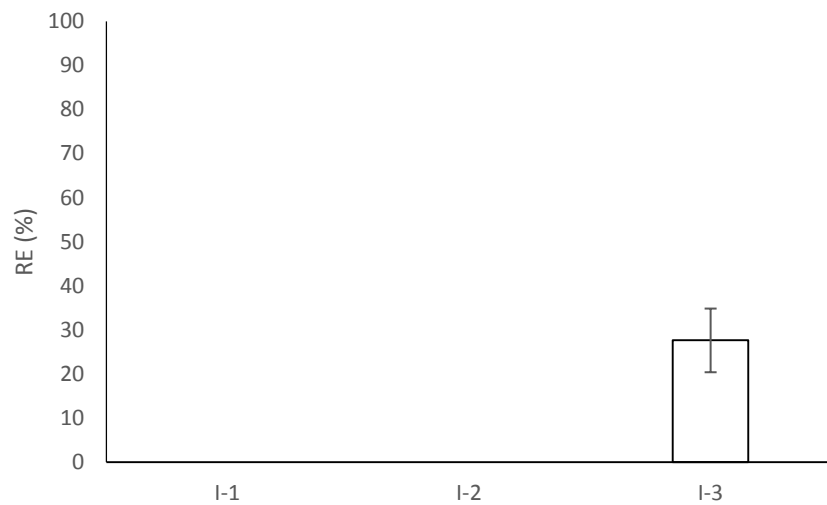


Figure 4. Steady state removal efficiencies of naproxen during phase A (a) and phase B (b). Vertical bar correspond to standard deviations from replicates.

a)



b)

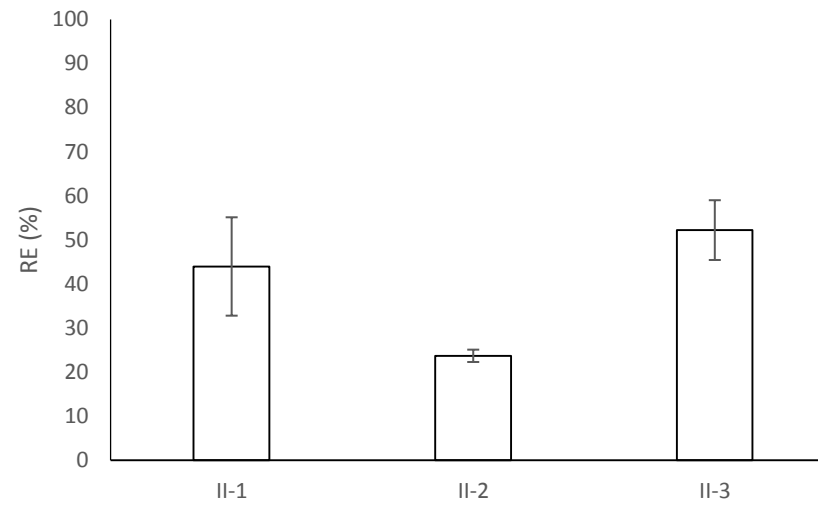
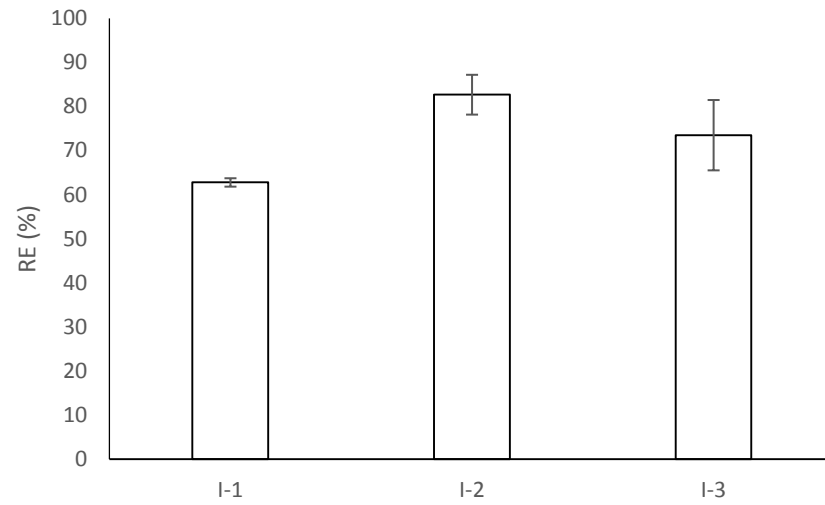


Figure 5. Steady state removal efficiencies of salicylic acid during phase A (a) and phase B (b). Vertical bar correspond to standard deviations from replicates.

a)



b)

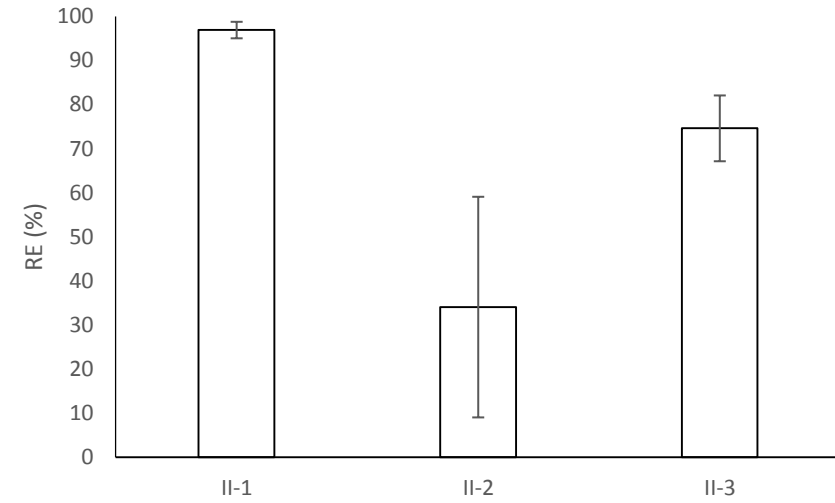
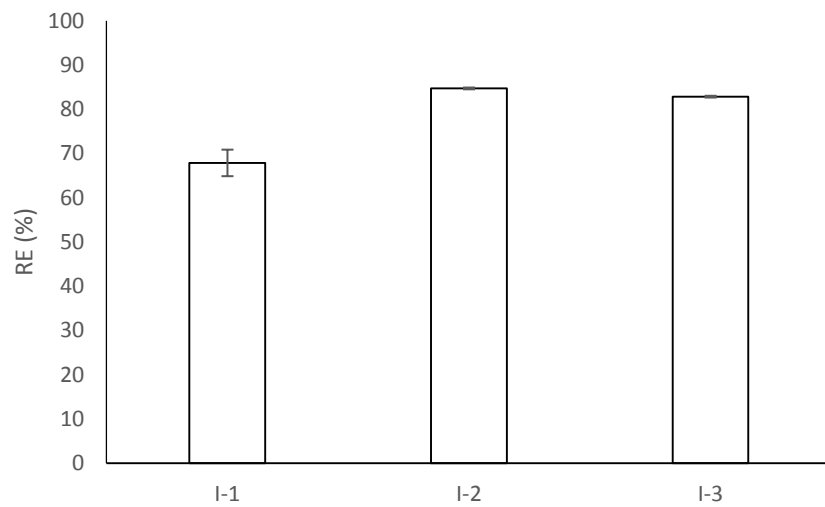


Figure 6. Steady state removal efficiencies of triclosan during phase A (a) and phase B (b). Vertical bar correspond to standard deviations from replicates.

a)



b)

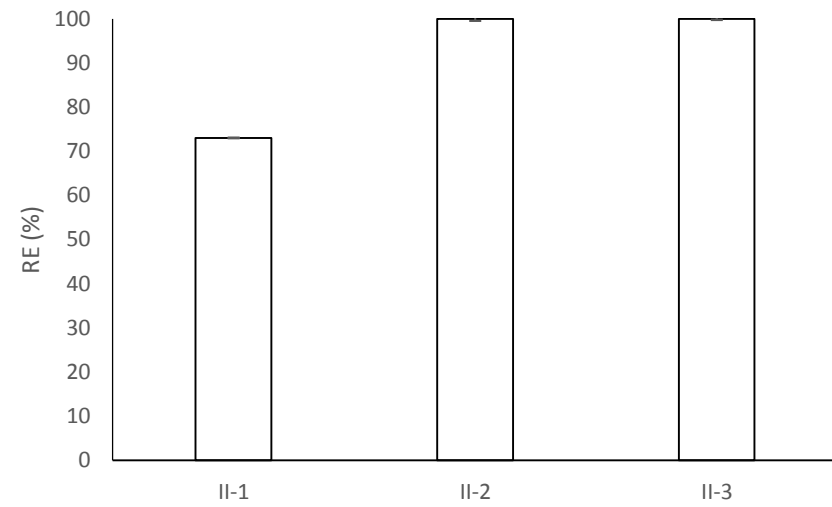
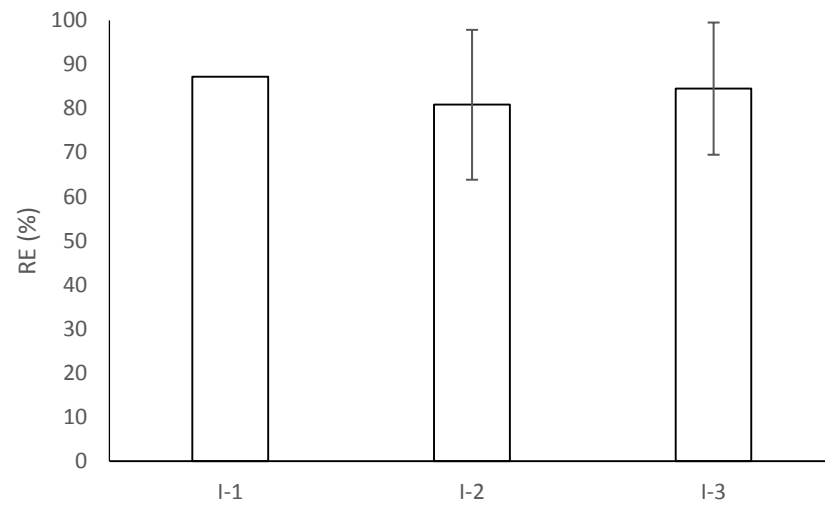
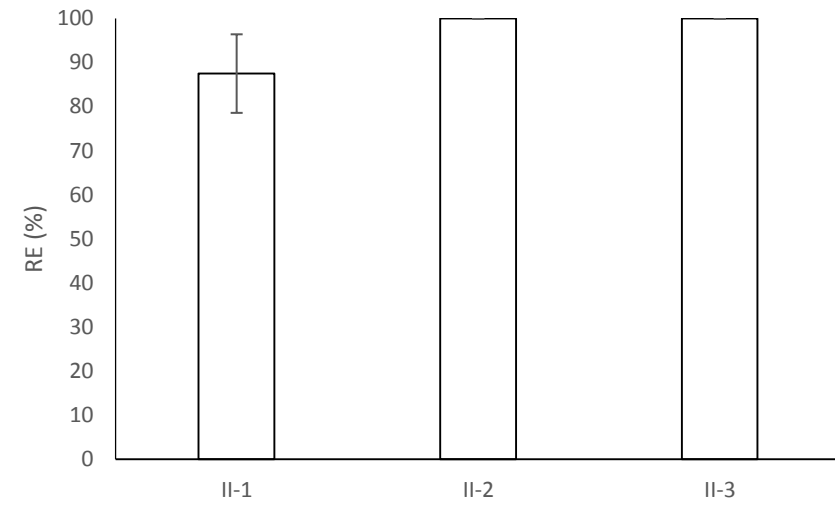


Figure 7. Steady state removal efficiencies of propylparaben during phase A (a) and phase B (b). Vertical bar correspond to standard deviations from replicates.

a)



b)



Supplementary material for on-line publication only

[Click here to download Supplementary material for on-line publication only: Supplementary data.docx](#)